Supplemental Figure 1

Metabolic flux with [U-^{13}C]Lactate - [^{12}C]Glutamine in primary hepatocytes

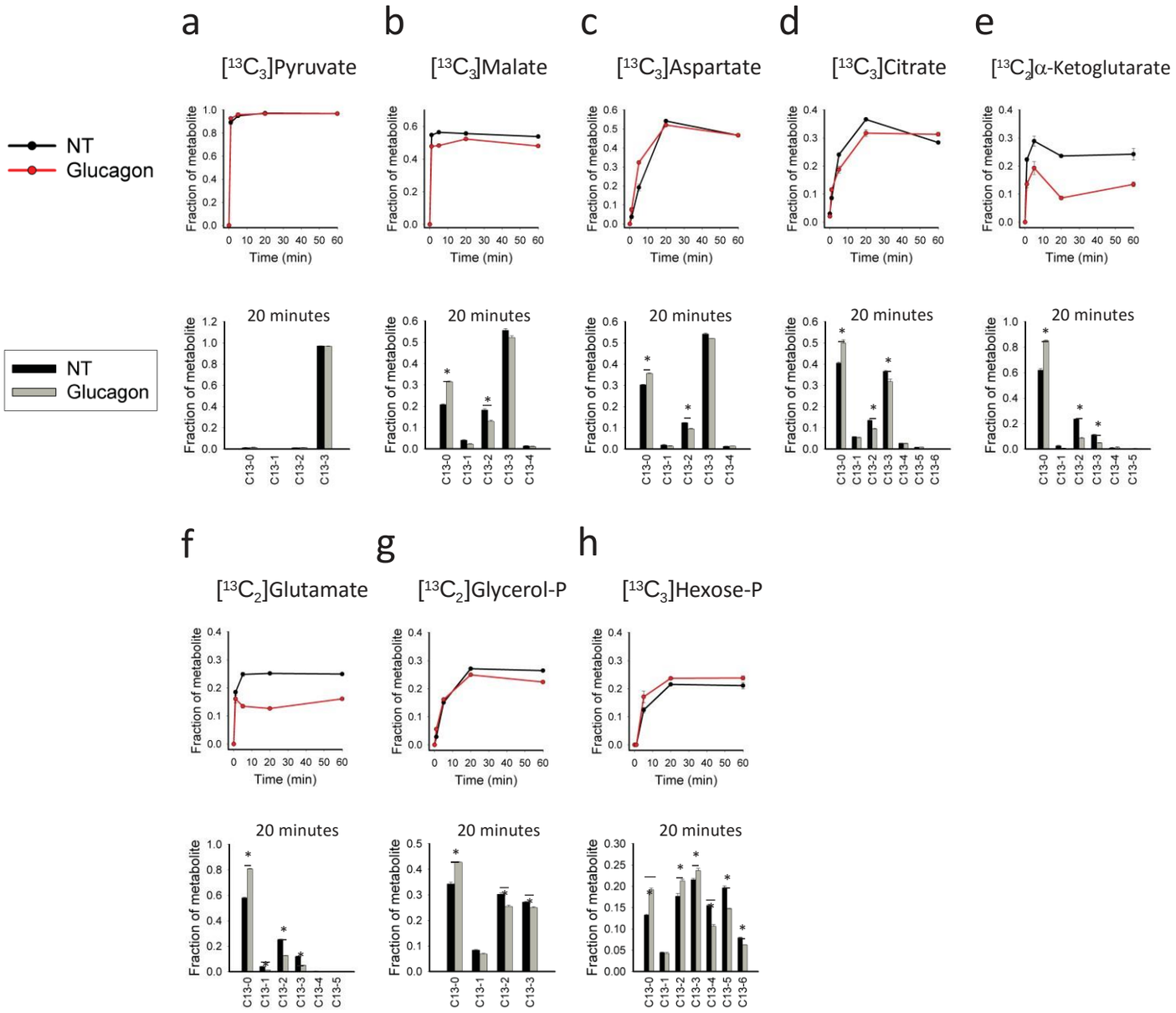

Supplemental figure 1. Metabolic flux with [U-^{13}C]Lactate - [^{12}C]Glutamine in primary hepatocytes (**a-h**) Primary isolated hepatocytes were treated with with [U-^{13}C]Lactate - [^{12}C]Glutamine and either PBS (NT) or glucagon and (**a**) [$^{13}C_3$]Pyruvate, (**b**) [$^{13}C_3$]malate, (**c**) [$^{13}C_3$]aspartate, (**d**) [^{13}C3]citrate, (**e**) [$^{13}C2_3$]α-ketoglutarate, (**f**) [$^{13}C_2$]glutamate, (**g**) [$^{13}C_2$]glycerol-phosphate, and (**h**) [$^{13}C_3$]hexose-phosphate. Top plots are kinetic timecourses following addition of glucagon. Bottom plots show the isotopomer distribution at the 20 minute time point.

Supplemental Figure 2

Metabolic flux with [^{12}C]Lactate - [U-^{13}C]Glutamine in primary hepatocytes

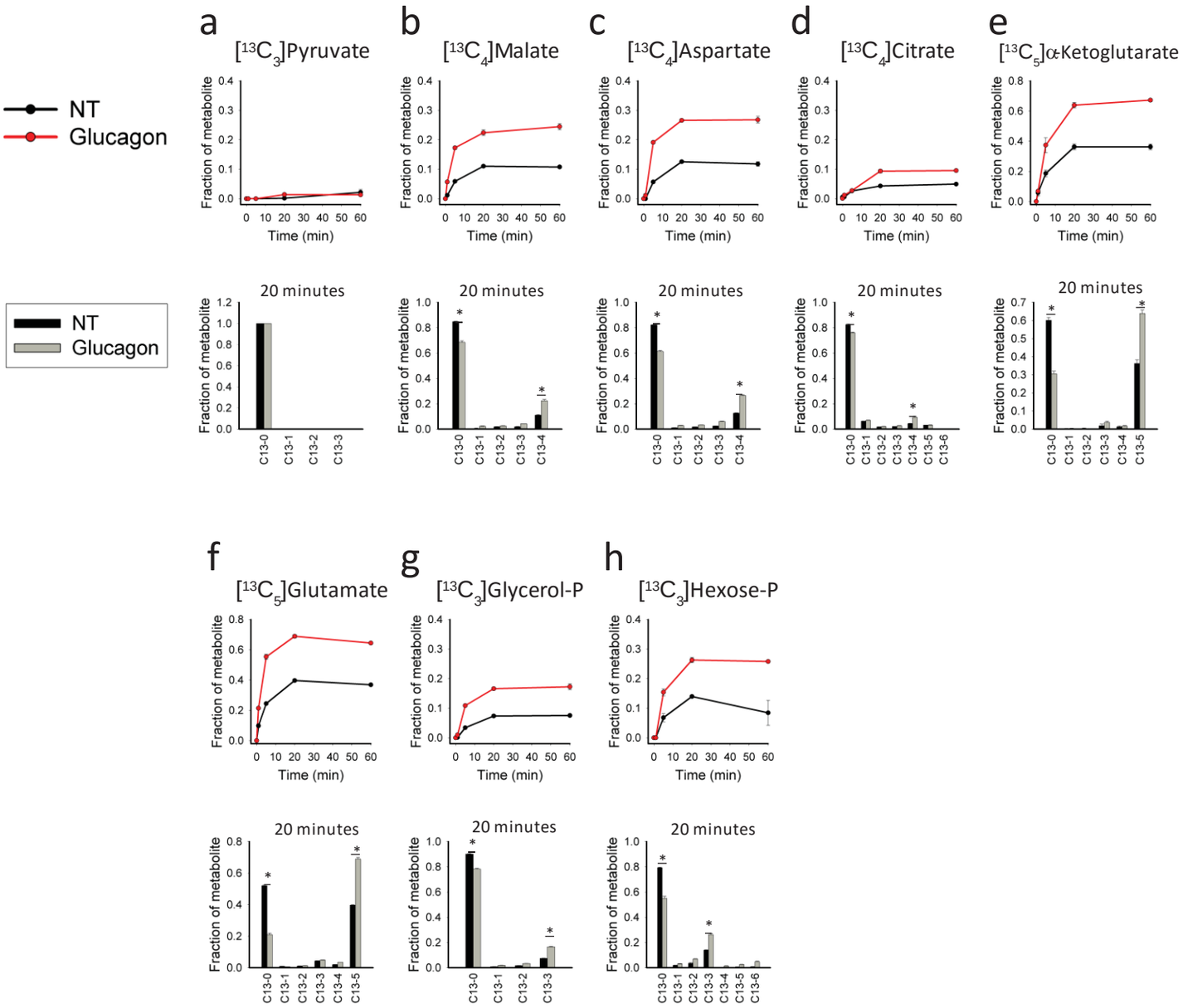

Supplemental figure 2. Metabolic flux with [^{12}C]Lactate - [U-^{13}C]Glutamine in primary hepatocytes (**a-h**) Primary isolated hepatocytes were treated with with [U-^{13}C]Lactate - [^{12}C]Glutamine and either PBS (NT) or glucagon and (**a**) [$^{13}C_3$]Pyruvate, (**b**) [$^{13}C_4$]malate, (**c**) [$^{13}C_4$]aspartate, (**d**) [$^{13}C_4$]citrate, (**e**) [$^{13}C_5$]α-ketoglutarate, (**f**) [$^{13}C_5$]glutamate, (**g**) [$^{13}C_3$]glycerol-phosphate, and (**h**) [$^{13}C_3$]hexose-phosphate. Top plots are kinetic timecourses following addition of glucagon. Bottom plots show the isotopomer distribution at the 20 minute time point.

Supplemental Figure 3

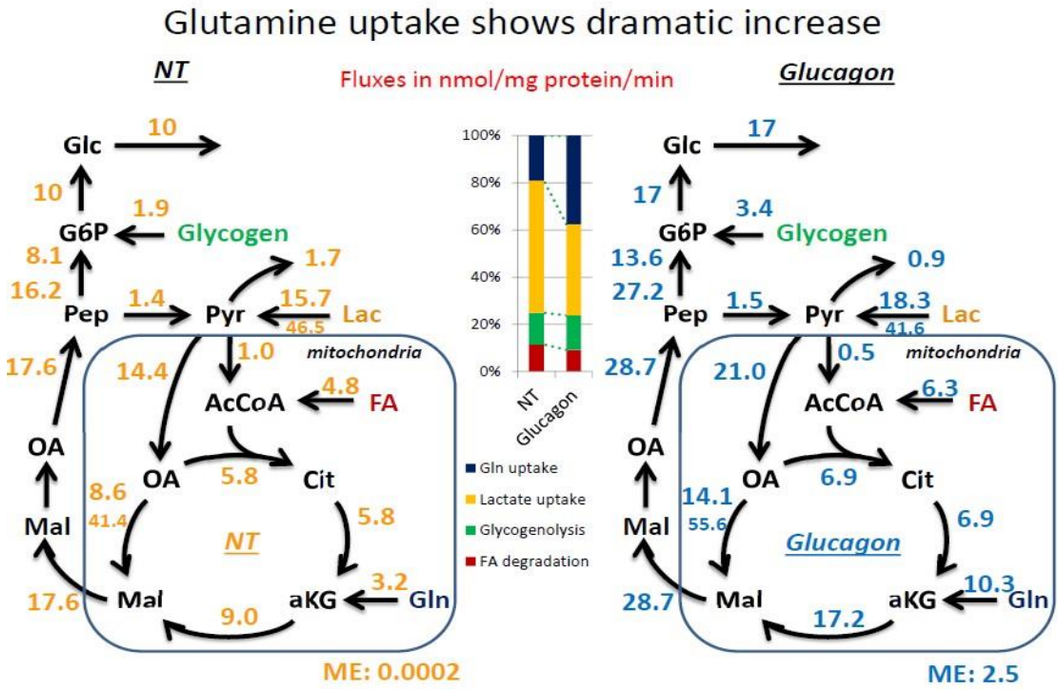

Supplemental figure 3. Modeling results from metabolic flux studies based on experiments presented in figure 1 and supplemental figures 1-2. Flux map with best fit flux values for untreated and glucagon stimulated fluxes.

Supplemental Figure 4

Intracellular glutamine in primary hepatocytes treated with glucagon

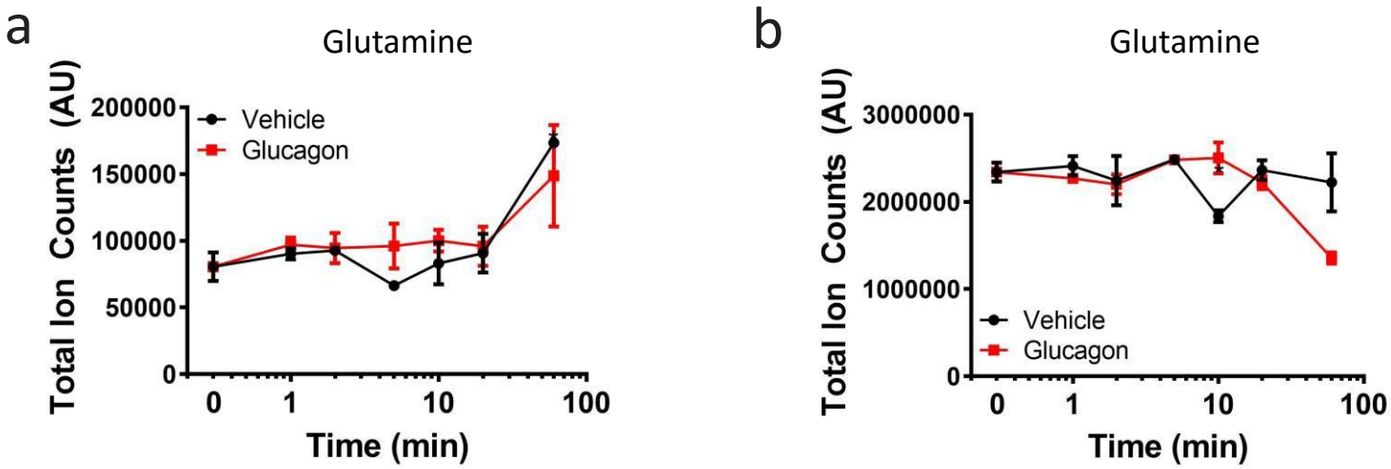

Supplemental figure 4. Intracellular glutamine in primary hepatocytes treated with glucagon or PBS vehicle. Primary hepatocytes were incubated with (**a**) lactate or (**b**) lactate and [$^{13}C_6$]glutamine and the intracellular glutamine was measured by mass spectrometry.

Supplemental Figure 5

Mechanistic and signaling studies in primary mouse hepatocyte

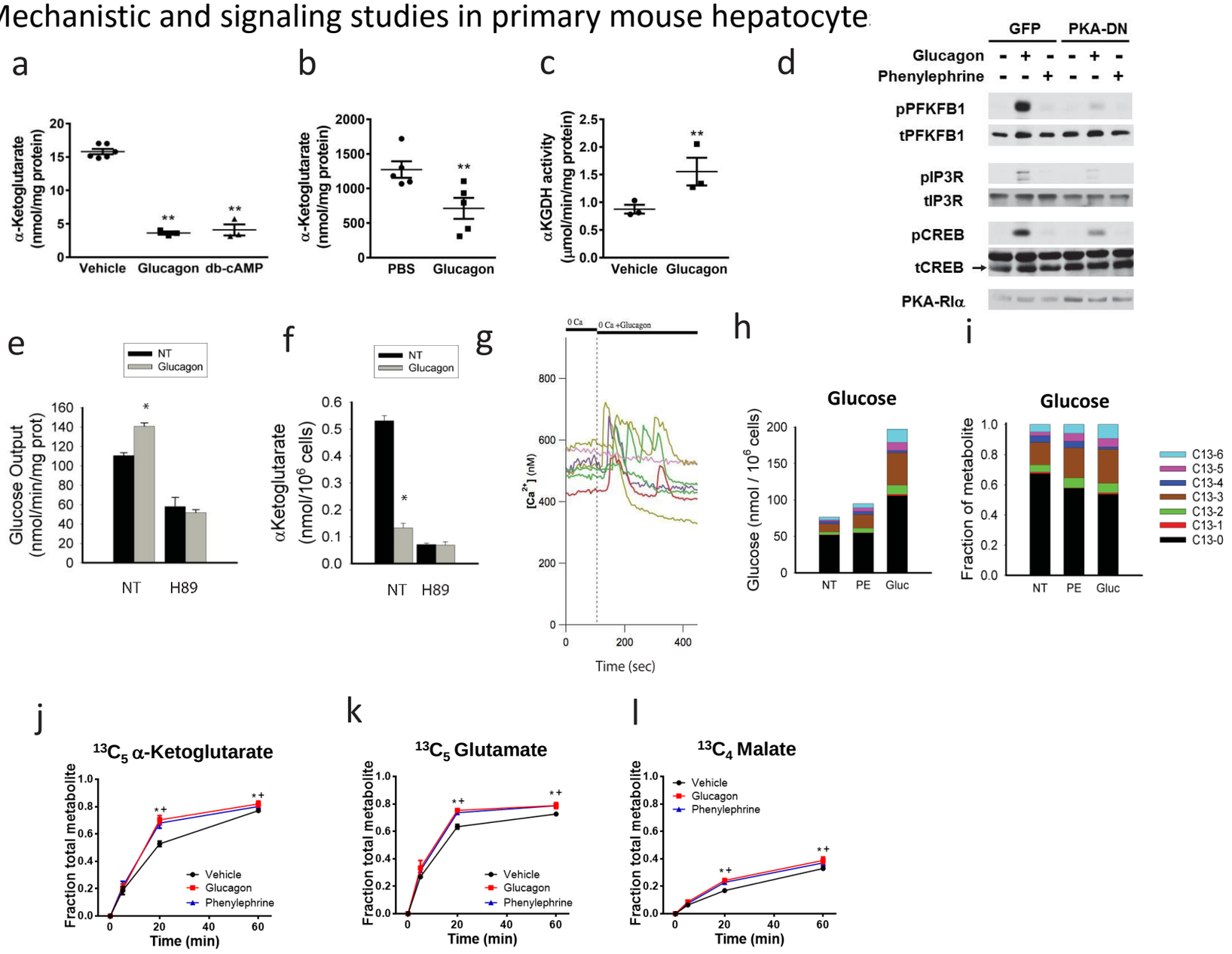

Supplemental figure 5. Mechanistic and signaling studies in primary mouse hepatocytes. (**a**) a-ketoglutarate levels following treatment of primary hepatocytes with PBS (vehicle), glucagon, or db-cAMP and measured enzymatically. (**b**) Liver a-ketoglutarate levels following treatment with a bolus injection of glucagon or PBS and and measured by mass spectrometry. (**c**) Measurement of a-kgdh enzymatic activity in primary hepatocytes treated with PBS or glucagon. (**d**) Primary hepatocytes isolated from mice infected with AAV-TBG-GFP or AAV-TBG-PKA-DN were isolated and treated with PBS, glucagon, or phenylephrine for 10 minutes and the resulting protein lysates were probed by western blot for phosphorylated or total Phosphofructokinase/FBPase1(PFKFB1), phosphorylated or total Inositol 3-Phosphate Receptor (IP3R), phosphorylated or total CREB, and the PKA regulatory subunit used to inhibit PKA activity (PKA-R1a). (**e-f**) Primary hepatocytes were treated with PBS (NT) or glucagon in the presence or absence of the PKA inhibitor H89 and (**e**) glucose output or (**f**) a-ketoglutarate levels were measured. (**g**) Primary hepatocytes were isolated and the levels of intracellular calcium were measured using calcium sensitive dyes in distinct hepatocytes. (**h-l**) Kinetic metabolic flux studies using [^{12}C]Lactate - [U-^{13}C]Glutamine in hepatocytes treated with PBS vehicle, glucagon, or phenylephrine were performed. The isotopomer pattern in extracellular glucose was measured and represented as a (**h**) total amount or (**l**) the fraction of the total glucose pool. Intracellular metabolite labeling patterns are shown for (**j**) [$^{13}C_5$]a-ketoglutarate, (**k**) [$^{13}C_5$]glutamate, and (**j**) [$^{13}C_4$]malate.

Supplemental Figure 6

Mechanistic and signaling studies in mouse liver

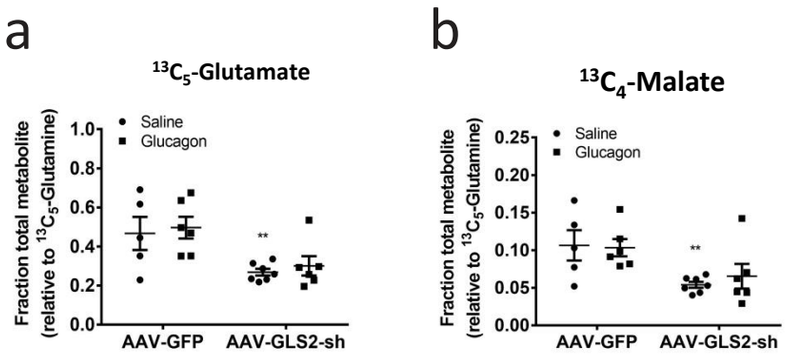

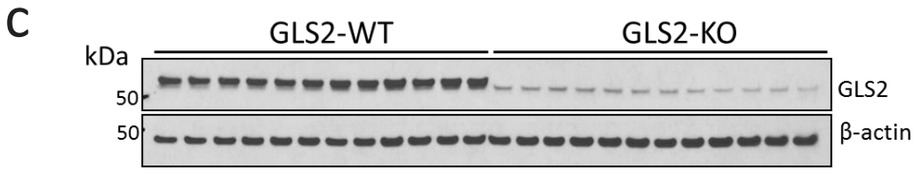

Supplemental figure 6. Mechanistic and signaling studies in mouse liver. (**a-b**) Animals infected with AAV-GFP or AAV-GLS2-sh were infused with [U-^{13}C]Glutamine and PBS vehicle or glucagon. Hepatic enrichment of (**a**) [$^{13}C_5$]glutamate and (**b**) [$^{13}C_4$]malate. Values are corrected for plasma enrichment of glutamine. (**c**) Western blot evaluation of GLS2 protein levels in livers from GLS2-KO and litter mate control animals.

Supplemental Figure 7
Original Scan of Western Blots

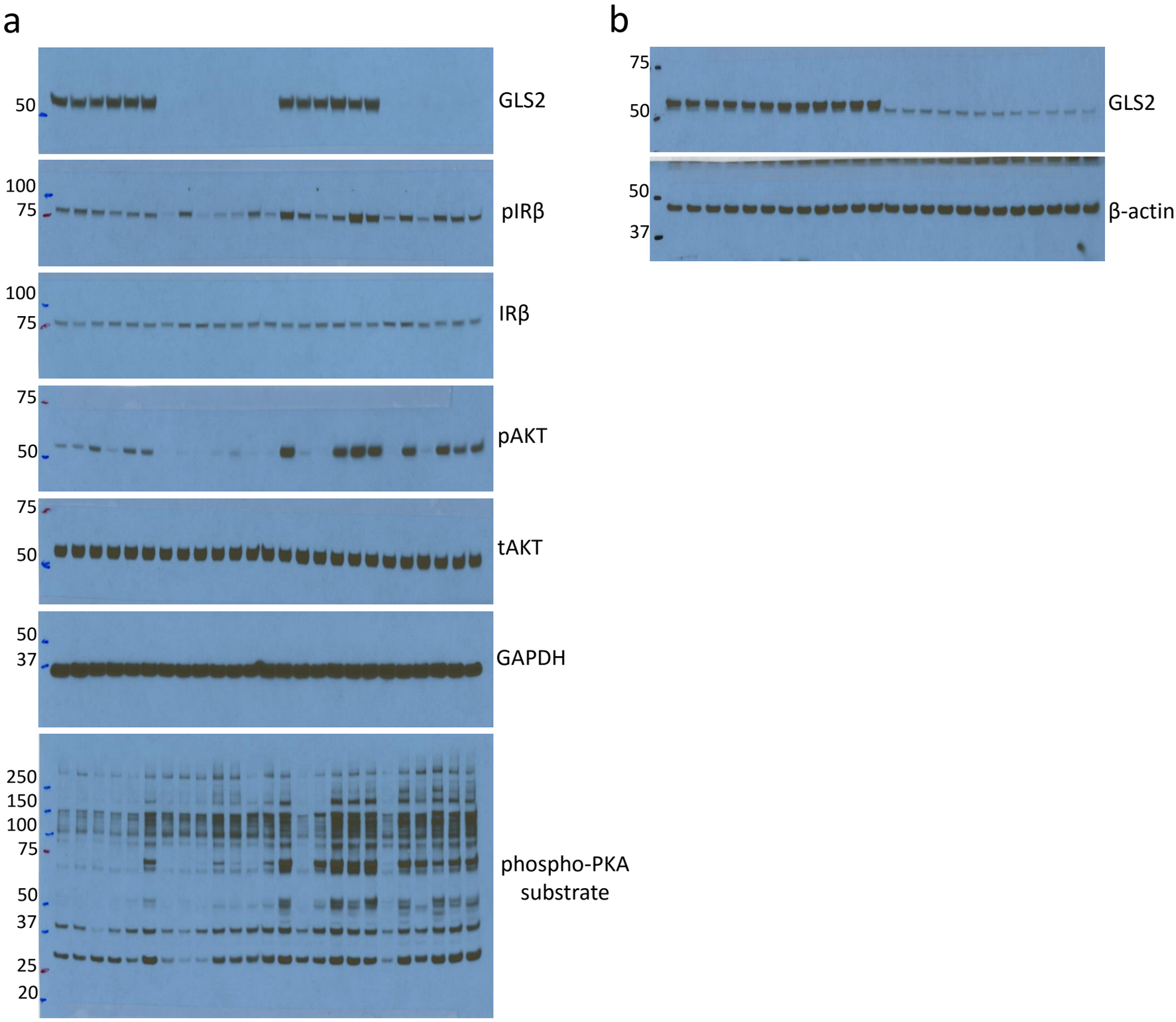

Supplemental Figure 8. Original Scan of Western Blots

A. Original Scan for figure 3a and supplemental figure 6a. **B**. Original Scan for supplemental figure 6d

Supplemental Table 1
Best fit fluxes and lower and upper bounds of modeling

	95% confidence interval		Basal			Glucagon	
	nmol/mg protein/min	LB	BEST	UB	LB	BEST	UB
Net	**Glc secretion**	9.5	10.0	10.0	16.0	17.0	17.5
Net	**Pyr secretion**	1.3	1.7	1.7	0.9	0.9	1.4
Net	**FA degradation**	4.4	4.8	5.5	5.9	6.3	6.8
Net	**Glycogenolysis**	1.6	1.9	1.9	3.1	3.4	3.7
Net	**Lactate uptake**	15.4	15.7	18.9	17.3	18.3	19.5
Net	**Gln uptake**	3.2	3.2	3.9	9.6	10.3	10.8
Net	**aKG→Succ-CoA+CO2**	8.4	8.9	10.3	16.0	17.2	17.7
Reverse	**aKG→Succ-CoA+CO2**	0.0	0.3	0.7	0.7	1.0	1.4
Net	**Ac-CoA+OA→Cit**	5.4	5.8	5.8	6.7	6.9	7.3
Net	**PEP+H2O→2PG**	16.2	16.2	16.8	26.6	27.2	27.7
Reverse	**PEP+H2O→2PG**	49.2	983.3	1000.0	0.0	0.0	0.1
Net	**GAP+DHAP→FBP**	8.1	8.1	8.4	13.3	13.6	13.9
Net	**2 Fum + 2 H2O → 2 Mal**	4.2	4.5	5.1	7.7	8.6	9.1
Net	**Lac→Pyr**	15.4	15.7	18.9	17.3	18.3	19.5
Net	**Mal→OA**	16.9	17.6	17.6	27.2	28.7	31.3
Net	**OA→Mal (mitochondria)**	8.6	8.6	11.3	13.1	14.1	15.1
Reverse	**OA→Mal (mitochondria)**	32.7	41.4	65.8	43.3	55.6	67.2
Net	**Mal→Pyr+CO2**	0.0	0.0	0.0	0.0	2.5	4.0
Net	**Pyr+CO2→OA**	14.4	14.4	16.6	19.5	21.0	22.2
Net	**Pyr→Ac-CoA+CO2**	0.9	1.0	1.3	0.4	0.5	0.6
Net	**PEP→Pyr**	0.6	1.4	1.4	0.0	1.6	5.0

Supplemental table 1. Best fit and upper/lower bounds from modeling results from metabolic flux studies based on experiments presented in figure 1 and supplemental figures 1-2.